

## Quantitative measurement of Cr segregation in $\text{Co}_{0.8-x}\text{Cr}_x\text{Pt}_{0.1}\text{B}_{0.1}$ recording media by scatter diagram analysis

Werner Grogger<sup>a)</sup> and Kannan M. Krishnan<sup>b)</sup>

*Materials Sciences Division, National Center for Electron Microscopy, Lawrence Berkeley National Laboratory, Berkeley, California 94720*

Roger A. Ristau, Thomas Thomson, Samuel D. Harkness, and Rajiv Ranjan

*Seagate Recording Media, 47010 Kato Road, Fremont, California 94538*

(Received 29 January 2001; accepted for publication 17 December 2001)

We describe the scatter diagram analysis of chemically resolved energy-filtered transmission electron microscopy (EFTEM) images and demonstrate its application in obtaining quantitative information about the segregation of Cr on the nanometer scale. The recording performance of Co–Cr based magnetic media depends critically on the microstructure of the thin film alloy, i.e., the degree of segregation of Cr to the grain boundaries determines the extent of magnetic isolation that can be achieved. Magnetic isolation of the grains reduces transition widths and thereby allows increased recording densities. The EFTEM results obtained correlate well with both the magnetic properties and recording performance of the media; i.e., a higher Cr content of 16 at. % (compared with a 10 at. % sample) shows substantial segregation of Cr with about 8% (0.06%) of the image area, most of it at the grain boundaries, having a Cr concentration which is higher than 24 at. %, and a medium signal to noise ratio of 17.8 dB (15.3 dB). © 2002 American Institute of Physics. [DOI: 10.1063/1.1450039]

The composition and processing of the Co–Cr alloy thin films, used as magnetic recording media, significantly influence their recording performance, particularly in terms of the medium signal to noise ratio (SMNR).<sup>1,2</sup> It is well known that compositional inhomogeneities in the medium are responsible for many of the desirable recording characteristics. Hence, understanding the medium microstructure and microchemistry, particularly the segregation of Cr to the grain boundaries in Co–Cr based recording media, is essential to obtain further improvements in medium performance. The regions between crystalline grains are believed to strongly affect the exchange coupling between magnetic grains. Ideally for maximum SMNR, one would wish to have completely exchange-decoupled, magnetically isolated grains acting as single domain particles. In Co–Cr alloys, segregation of Cr to regions between the grains would naturally lead to such a microstructure provided the Cr enrichment is sufficiently high as to render the local Co–Cr composition nonmagnetic in the temperature range of interest, i.e., 280–340 K. Further, if the magnetic grains are surrounded by a thin nonmagnetic layer of this Cr-rich alloy, true isolation would result leading to a significant reduction in media noise. Therefore, it is critically important to not only measure the amount of Cr at the grain boundaries but also sample a large number of such boundaries in a single measurement to provide statistically significant results.

The lateral resolution required of any such quantitative measurement is quite small: the diameters of the grains used

in high recording density media typically lie in the 10 nm range and the Cr segregation region at the grain boundaries is on the subnanometer scale. Numerous experimental methods have been applied to explore these Co–Cr alloy microstructure and microchemistry, including nuclear magnetic resonance,<sup>3</sup> atom probe field ion microscopy,<sup>4</sup> and analytical transmission electron microscopy (TEM).<sup>5–11</sup> In a modern TEM one can use a fine probe ( $\sim 1$  nm diameter) with a high current density ( $\sim 0.5$  nA/nm<sup>2</sup>), stepping it across the region of interest, and acquiring either energy dispersive x-ray spectrometry or electron energy-loss spectrometry (EELS) data at each point. In most cases this technique is tedious as it only yields a linear array of data.

An alternative technique involving spatially resolved measurements of characteristic inner-shell excitations in EELS (energy-filtering TEM or EFTEM)<sup>7–9</sup> is a powerful method for exploring the chemical microstructure of inhomogeneous alloy recording media. Using EFTEM has the advantage of simultaneously acquiring quantitative element-specific data from the entire image area with a spatial resolution below 1 nm.<sup>12,13</sup> However, the question remains on how to extract representative information about Cr segregation from these elemental maps or images. Usually, data extraction has been performed by drawing line profiles integrated over a certain number of pixels. The integration reduces noise but requires straight interfaces, which in many cases are rather hard to find in a statistically significant number. However, the data are only one dimensional and for statistically meaningful results a large number of such line profiles must be analyzed.

Alternatively, other analysis methods can be applied which actually take advantage of the complete two-dimensional data set in an EFTEM image. In particular, scatter diagram analysis has proven to be an effective method for

<sup>a)</sup>Now at: FELMI, Technical University Graz, Steyregasse 17, A-8010 Graz, Austria; electronic mail: werner.grogger@felmi-zfe.at

<sup>b)</sup>Author to whom correspondence should be addressed; now at: Dept. of Materials Science, Univ. of Washington, Seattle, WA 98195; electronic mail: kannanmk@u.washington.edu

TABLE I. Magnetic and recording performance data from VSM, RDM, and spinstand measurements. The  $S^*r$  and SFD<sub>r</sub> were derived from dcd remanence curves. The SFD<sub>r</sub> is the full width half maximum of the differentiated dcd remanence curve normalized to the remanent coercivity.

Sample	$H_{cr}$ (Oe)	$M_s$ (emu/cm <sup>3</sup> )	$M_{r,t}$ (memu/cm <sup>2</sup> )	$S^*r$	SFD <sub>r</sub>	SMNR (dB)	PW50 (nm)
10% Cr	4023	370	0.39	0.80	0.23	15.3	135
16% Cr	4518	300	0.37	0.84	0.26	17.8	132

extracting quantitative data from images.<sup>13,14</sup> In this work, the quantitative statistical analysis of EFTEM elemental maps using scatter diagrams is applied to measure the segregation of Cr in CoCrPtB alloys. This letter describes quantitative results that relate magnetic recording performance to changes in the medium microstructure due to variation of Cr concentration.

Two CoCrPtB magnetic thin film media were sputtered on aluminum substrates using a standard commercial dc magnetron sputtering system. The films had similar underlayer/interlayer/magnetic layer structure but with differing amounts of Cr in the magnetic alloy. The compositions of the two films were both CoCrPtB, but the Co/Cr concentration ratio of one sample was 70/10 and the second 64/16 atom percent while the Pt and B content were the same (~10 at. %) for both.

The recording performance measurements were made using a Guzik 1701 spinstand equipped with a 10 Gbit/in.<sup>2</sup> type head at linear densities up to 500 kfc/i. Basic magnetic properties ( $H_{cr}$ ,  $M_s$ ,  $M_{r,t}$ ,  $S^*r$ ) were measured using a digital measurement system vibrating sample magnetometer (VSM) at a maximum field of  $\pm 15$  kOe and an in-house rotating disk magnetometer (RDM). Isothermal and d.c. demagnetizing (dcd) remanence curve data for the  $\Delta M$  plots were taken using a Princeton Measurement Corporation alternating gradient force magnetometer. All magnetic properties were measured at room temperature.

Plan-view specimens for TEM of both samples were prepared using conventional preparation techniques including mechanical polishing, dimpling and ion milling. The TEM investigations were performed on a Philips CM200/FEG operated at 200 kV. All energy-filtered images, using characteristic inner shell excitations in electron energy-loss spectroscopy (Co  $L_{23}$  and Cr  $L_{23}$  edges, i.e.,  $2p$  to unoccupied  $3d$  transitions following dipole selection rules) were acquired with a Gatan imaging filter. Elemental maps were calculated using the three-window technique.<sup>15</sup> However, small amounts of oxygen, due to the surface oxidation of the alloy thin film samples, made it necessary to apply a four-window technique in the case of Cr in order to perform a reliable quantification.<sup>8</sup> The window positions were 500/520/557/593 eV for Cr and 731/761/-/797 eV for Co (pre1/pre2/pre3/postedge window), and a slit width of 30 eV was used. The exposure times were between 15 and 30 s.

There are additional constraints in the observable EFTEM signal strength arising from the optimization of the media for recording purposes. As the magnetically active recording layer is thin (~15 nm) it provides only a small number of scattering atoms (around 100–200 Cr atoms per nm<sup>2</sup>) and the available signals are rather weak (typically 200–

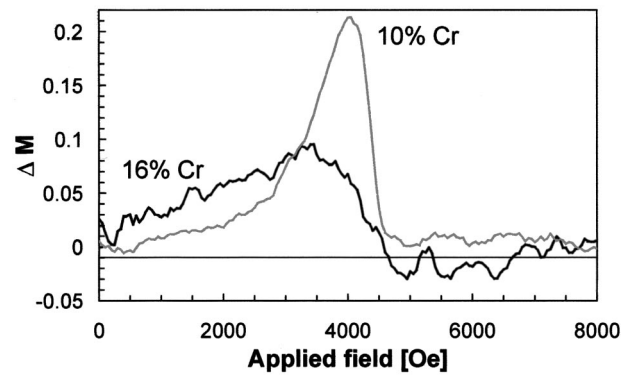


FIG. 1.  $\Delta M$  curves for two 10% Cr and 16% Cr CoCrPtB alloys.

1000 net counts in the elemental maps). Therefore, a low-pass filter was applied to all maps before further quantitative analysis. As the thickness of both specimens was uniform throughout the images, quantification was simply done by normalizing gray values of the elemental maps to the nominal concentrations.

For the statistical analysis of the data scatter diagrams were used (for a detailed description see Refs. 13 and 14 and references therein). A scatter diagram can be considered as a two-dimensional histogram showing the frequency of occurrence of gray value combinations of two elemental distribution images. In the case of a correlation between the two, one, or more clusters can be seen in the scatter diagram, each indicating a different gray value combination. These clusters can be related to different chemical phases, when element sensitive images (e.g., elemental maps) are used as input. Furthermore, the clusters can be mapped back to find the image areas where they originate from to create chemical phase images.

Spin stand data of the recording performance show a significant difference in the two samples, particularly in SMNR, Table I. A difference in SMNR of 2.5 dB indicates that the low Cr alloy (10 at. % Cr) has significantly greater medium noise than the high Cr alloy (16 at. % Cr). The  $\Delta M$  curves shown in Fig. 1 indicate a significant difference in coupling for the two media. A positive  $\Delta M$  plot results from a system where interactions that resist magnetization reversal dominate. In polycrystalline thin film media this is due to exchange coupling between grains.<sup>16</sup> A negative  $\Delta M$  plot indicates that demagnetizing or magnetostatic interactions prevail. The data in Fig. 1 clearly demonstrate that exchange coupling is significantly reduced in the case of the sample with 16 at. % Cr compared with that of the 10 at. % Cr media. This is also consistent with the switching field distribution (SFD<sub>r</sub>) parameter  $S^*r$  (Table 1) where the more highly exchange coupled medium leads to a narrower SFD<sub>r</sub>.

Figure 2 shows the EFTEM results for the 16 at. % Cr alloy. Due to different diffracting conditions, only a few grains are visible in the bright field image [Fig. 2(a)]. The elemental maps of Co and Cr in Figs. 2(b) and 2(c) show the effect of the Cr segregation to the grain boundaries; clearly, Cr is enriched whereas Co is depleted. The scatter diagram [Fig. 2(d)] confirms the expected inverse correlation between the Co and Cr distributions as an elongated cluster along its diagonal. Additionally, it only shows *one* cluster indicating a

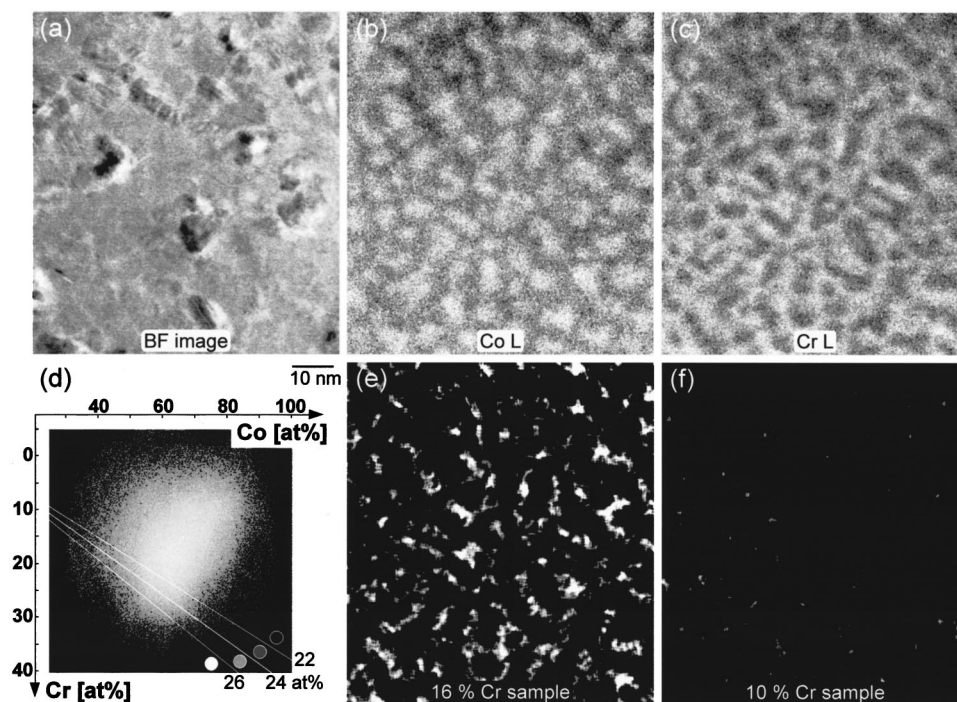


FIG. 2. EFTEM images of a CoCrPtB alloy with 16 at. % Cr. (a) TEM bright field image. The elemental maps of the Co  $L_{23}$  (b) and Cr  $L_{23}$  (c) ionization edges show the Cr enrichment along the grain boundaries and in the center of some grains. Using quantified elemental maps calculated from (b) and (c) a two-dimensional scatter diagram (d) was calculated. The scatter diagram clearly indicates an inverse relationship between Co and Cr and a continuous variation of both elements. Using lines at certain Co/Cr atomic ratios the scatter diagram was segmented into regions of different Cr contents. From these regions a trace back was computed for both samples [16% Cr: (e) and 10% Cr: (f)], showing regions with the same Cr content in the same shade of gray [see corresponding circles in (d)].

continuous compositional variation of Co and Cr between the grains.

In this case, lines representing specific Co/Cr ratios were used to segment the scatter diagram into various regions, each of them corresponding to a certain compositional range (<22 at. %, 22–24 at. %, 24–26 at. %, >26 at. %; shown in different shades of gray). Such segmentation lines representing specific Co/Cr ratios take care of effects responsible for the broadening of the cluster (noise, diffraction contrast). Finding the areas in the elemental maps that contribute to specific regions in the scatter diagram leads to a “phase map,” where each phase again corresponds to a certain composition. In Figs. 2(e) and 2(f) these phases are shown with the corresponding shades of gray of Fig. 2(d). It should be noted that the different phases do not correspond to real chemical phases, they only show different compositional ranges. In Figs. 2(e) and 2(f) the phase maps for the two alloys are shown, clearly indicating the different amount of Cr segregating to the grain boundaries. For the 16 at. % Cr sample most of the grains are at least partially surrounded by material with 24 at. % Cr or more (bright areas). The 10 at. % Cr sample shows a completely different picture: only a few areas with high Cr concentration can be seen. The results for the two alloys can be easily compared in terms of the area percentage for each compositional range. In the case of the 16 at. % Cr alloy about 8% of the image area, almost all of it at the grain boundaries, has a Cr concentration of 24 at. % or more, whereas this value is much less for the 10 at. % Cr alloy (0.06%).

Two CoCrPtB alloys with different Cr content were investigated quantitatively using EFTEM, magnetization measurements, and recording performance data. The alloy with greater Cr content (16 at. %) showed an increased amount of Cr that segregated to the grain boundaries. The higher Cr content alloy had a greater SMNR due to the more effective magnetic isolation of grains. The decrease in intergranular exchange coupling was confirmed by  $\Delta M$  measurements.

W.G. acknowledges support from the Max Kade Foundation for his stay at Berkeley. Work at LBNL/NCM was supported by the Director, Office of Energy Research, Office of Basic Energy Sciences, Materials Sciences Division of the U.S. Department of Energy under Contract No. DE-AC03-76SF00098. E. C. Nelson is gratefully acknowledged for assistance with the CM200 operation.

- <sup>1</sup>M. F. Doerner, T. Yogi, D. S. Parker, S. Lambert, B. Hermsmeier, O. C. Allegranza, and T. Nguyen, *IEEE Trans. Magn.* **29**, 3667 (1993).
- <sup>2</sup>T. Keitoku, J. Ariake, N. Honda, K. Ouchi, and S. Iwasaki, *J. Magn. Mater.* **176**, 25 (1997).
- <sup>3</sup>K. Yoshida, H. Kakibayashi, and H. Yasuoka, *Mater. Res. Soc. Symp. Proc.* **232**, 47 (1991).
- <sup>4</sup>K. Hono, Y. Maeda, J. L. Li, and T. Sakurai, *IEEE Trans. Magn.* **29**, 3745 (1993).
- <sup>5</sup>Y. Yahisa, K. Kimoto, K. Usami, Y. Matsuda, J. Inagaki, K. Furusawa, and S. Narishige, *IEEE Trans. Magn.* **31**, 2836 (1995).
- <sup>6</sup>Y. Hirayama, M. Futamoto, K. Kimoto, and K. Usami, *IEEE Trans. Magn.* **32**, 3807 (1996).
- <sup>7</sup>J. E. Witting, T. P. Nolan, R. A. Ross, M. E. Schabes, K. Tang, R. Sinclair, and J. Bentley, *IEEE Trans. Magn.* **34**, 1564 (1998).
- <sup>8</sup>J. Bentley, J. E. Witting, and T. P. Nolan, *Mater. Res. Soc. Symp. Proc.* **517**, 205 (1998).
- <sup>9</sup>M. Takahashi, A. Kikuchi, J. Nakai, and H. Shoji, *J. Magn. Mater.* **193**, 79 (1999).
- <sup>10</sup>M. Futamoto, N. Inaba, Y. Hirayama, K. Ito, and Y. Honda, *J. Magn. Mater.* **193**, 36 (1999).
- <sup>11</sup>N. Inaba and M. Futamoto, *J. Appl. Phys.* **87**, 6863 (2000).
- <sup>12</sup>*Energy-Filtering Transmission Electron Microscopy*, edited by L. Reimer (Springer, Berlin, 1995).
- <sup>13</sup>F. Hofer, W. Grogger, G. Kothleitner, and P. Warbichler, *Ultramicroscopy* **67**, 83 (1997).
- <sup>14</sup>W. Grogger, F. Hofer, and G. Kothleitner, *Mikrochim. Acta* **125**, 13 (1997).
- <sup>15</sup>O. L. Krivanek, A. J. Gubbens, M. K. Kundmann, and G. C. Carpenter, in *Proceedings of the 51st Annual Meeting Microscopy Society of America*, edited by G. W. Bailey and C. L. Rieder (San Francisco Press, San Francisco, 1993), p. 586.
- <sup>16</sup>P. I. Mayo, K. O'Grady, R. W. Chantrell, J. A. Cambridge, I. L. Sanders, T. Yogi, and J. K. Howard, *J. Magn. Mater.* **95**, 109 (1991).